[7] Fox, J. H., "On the Structure of Jet Plumes," *AIAA Journal*, Vol. 12, Jan. 1974, pp. 105–107.
[8] Chang, I. S. and Chow, W. L., "Mach Disc from Underexpanded Axisymmetric Nozzle Flow," *AIAA Journal*, Vol. 12, Aug. 1974, pp. 1079–1082.
[9] Chow, W. L. and Chang, I. S., "Mach Reflection from Overexpanded Nozzle Flows," *AIAA Journal*, Vol. 10, Sept. 1972, pp. 1261–1263.
[10] Traugott, S. C., "An Approximate Solution of the Direct Supersonic Blunt Body Problem for Arbitrary Axisymmetric Shapes," *Journal of the Aerospace Science*, Vol. 27, May 1960, pp. 361–370.
[11] Buseman, A., "A Review of Analytical Methods for the Treatment of Flows with Detached Shocks," TN 1858, 1949, NACA.
[12] Sternberg, J., "Triple-Shock-Wave Interactions," *The Physics of Fluids*, Vol. 2, Feb. 1959, pp. 179–206.
[13] Guderley, K. G., *The Theory of Transonic Flow*, Pergamon, Addison-Wesley, Reading, Mass., 1962, pp. 144–149.
[14] Ferri, A., *Elements of Aerodynamics of Supersonic Flows*, Macmillan, New York, 1949, pp. 177.
[15] Love, E. S. and Grigsby, C. E., "Some Studies of Axisymmetric Free Jets Exhausting from Sonic and Supersonic Nozzles into Still Air and into Supersonic Streams," RM L43L31, May 1958, NACA.

JUNE 1975 AIAA JOURNAL VOL. 13, NO. 6

Hydrodynamic Stability of the Far Wake of a Hovering Rotor

BHARAT P. GUPTA*
Bell Helicopter Co., Fort Worth, Texas
AND
MARTIN LESSEN†
University of Rochester, Rochester, N.Y.

The stability of a continuous model for the far wake of a hovering rotor has been formulated and analyzed. In the continuous model representation of the far wake, the vorticity of the interdigitated circular vortex helices is assumed to be distributed over a vortex sheet, and the potential flow inside and outside of the vortex sheet is taken to correspond to the average velocity profiles calculated for an interdigitated representation. A continuum of instabilities is found to exist for all wave numbers and for all modes except in some specific situations where the flow is neutrally stable. This model gives the instabilities of the gross flow and complements the interdigitated analysis of Ref. 1 which is the companion analysis for the instabilities of centerline displacements of the vortex helices.

Introduction

A STABILITY analysis of an interdigitated trailing vortex model of a hovering rotor for centerline displacement type of perturbations has been carried out by Gupta and Loewy.[1] The stability of the gross flow in the far wake of a hovering rotor, however, may be studied in a manner similar to that used by Lessen et al.[2] and by Uberoi[3] in their studies of trailing line vortices and jets.

By far wake, we mean the portion of the wake which is influenced by the vortex elements approximately one helix revolution away from the rotor, and where the induced effects of the lifting line vortex representation are insignificant. The reason for restricting the analysis to the far wake is that in the near wake, the lifting line has a stabilizing effect and therefore the near wake is expected to be more stable than the far wake. The relative stability of the near wake has been demonstrated by experimental rotor wake visualization studies and by theoretical free wake analyses where distortions of the wake due to induced velocities are considered.

Received May 20, 1974; revision received December 6, 1974.
Index category: Rotary Wing Aerodynamics.

* Research Engineer, Aeroacoustics; formerly a graduate student in the Department of Mechanical and Aerospace Sciences, University of Rochester, Rochester, N.Y.
† Professor, Department of Mechanical and Aerospace Sciences.

The far wake stability problem is important for several reasons, the most important one being the persistence of the wake of a hovering rotorcraft in the atmosphere and the pitching moments experienced by another aircraft flying into this wake. In such situations one might be interested to know the modal instabilities of the wake to arbitrarily small perturbations introduced by atmospheric disturbances and turbulence.

Another important reason concerns the numerical stability of the free wake type of analyses which are frequently used and which are found to be unsatisfactory in most hovering situations.

Finally, viscosity effects in the following analysis have been neglected because of the high Reynolds number associated with the flows. Reynolds numbers associated with the flows are of the order of 10^5–10^7 in most practical operating situations, and stability analyses of jets and wakes have indicated that viscous damping effects are negligible for Reynolds numbers greater than 50. In addition, it has been found that "top-hat" velocity and vorticity distributions, as representing actual jet and vortex combinations, have yielded stability results in good agreement with calculations of more accurate flowfield representations.

Velocity Profiles in the Far Wake

The far wake of a hovering helicopter can be represented by doubly infinite circular concentric helical vortices trailing from the root and tip of each blade. The details of induced velocity

calculations are given in Ref. 1. The cylindrical polar velocity components can be written down as

$$U_r = 0$$

$$\frac{2\Pi r U_\Phi}{\Gamma} = \sum_{m=1}^{n} k \int_o^x \frac{[R-\cos(x+\Psi_m)-x\sin(x+\Psi_m)]}{[1+R^2-2R\cos(x+\Psi_m)+k^2x^2]^{3/2}}\,dx$$

$$\frac{2\Pi r U_z}{\Gamma} = \sum_{m=1}^{n} \int_o^\infty \frac{[1-R\cos(x+\Psi_m)]}{[1+R^2-2R\cos(x+\Psi_m)+k^2x^2]^{3/2}}\,dx \qquad (1)$$

where (U_r, U_ϕ, U_z) = cylindrical polar velocity components, k = pitch of the helix, Γ = circulation of each vortex, n = number of vortices (also the number of blades), $R = r'/r$ radial distance normalized with respect to radius r of helix, x is running variable corresponding to azimuthal variable along the helix, and Ψ_m is the phase difference parameter in the same units. Numerical calculations of velocity components U_r, U_ϕ, U_z were carried out for systems of one through six interdigitated vortices and in each case the circumferential velocity was found to be proportional to $1/r$ and axial velocity was found to be a constant both exterior and interior of the vortex helices. A sample calculation of the velocity components for a system of six helices is shown in Fig. 1.

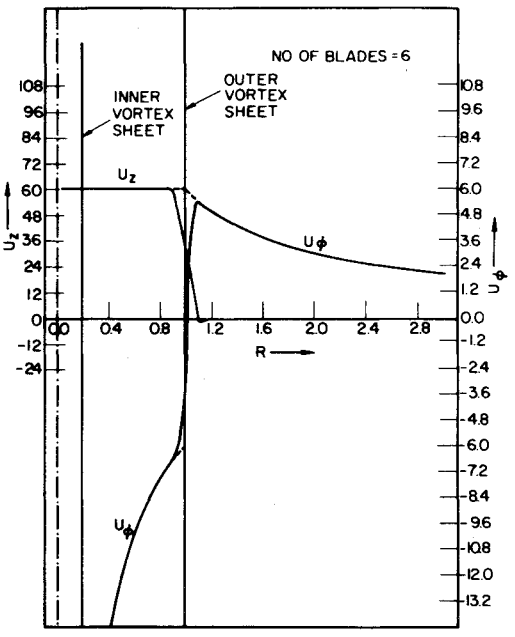

Fig. 1 Steady velocity profiles for the interdigitated wake model of a six-bladed rotor.

Differential Equation

The continuity and momentum equations for inviscid incompressible flow in cylindrical polar coordinates are

$$\frac{\partial v_r}{\partial r} + \frac{v_r}{r} + \frac{1}{r}\frac{\partial v_\phi}{\partial \phi} + \frac{\partial v_z}{\partial z} = 0 \quad \text{(continuity)}$$

$$\rho\left[\frac{\partial v_r}{\partial t} + v_r\frac{\partial v_r}{\partial r} + \frac{v_\phi}{r}\frac{\partial v_r}{\partial \phi} + v_z\frac{\partial v_r}{\partial z} - \frac{v_\phi^2}{r}\right] = -\frac{\partial p}{\partial r}$$

$$\rho\left[\frac{\partial v_\phi}{\partial t} + v_r\frac{\partial v_\phi}{\partial r} + \frac{v_\phi}{r}\frac{\partial v_\phi}{\partial \phi} + v_z\frac{\partial v_\phi}{\partial z} + \frac{v_r v_\phi}{r}\right] = -\frac{1}{r}\frac{\partial p}{\partial \phi}$$

$$\rho\left[\frac{\partial v_z}{\partial t} + v_r\frac{\partial v_z}{\partial r} + \frac{v_\phi}{r}\frac{\partial v_z}{\partial \phi} + v_z\frac{\partial v_z}{\partial z}\right] = -\frac{1}{r}\frac{\partial p}{\partial z} \qquad (2)$$

where velocity $\mathbf{v} = (v_r, v_\phi, v_z)$, ρ = density, and p = pressure.

If the dependent variables are now defined as having steady and perturbation parts such as

$$\begin{aligned} v_r &= u_r(r,\phi,z,t) \\ v_\phi &= U_\phi(r) + u_\phi(r,\phi,z,t) \\ v_z &= U_z(r) + u_z(r,\phi,z,t) \\ p &= P(r) + p(r,\phi,z,t) \end{aligned} \qquad (3)$$

Where the steady parts $U_\phi(r)$, $U_z(r)$, $P(r)$ in themselves satisfy the continuity and momentum equations, the first order (linear) equations for the perturbation become

$$\frac{\partial u_r}{\partial r} + \frac{u_r}{r} + \frac{1}{r}\frac{\partial u_\phi}{\partial \phi} + \frac{\partial u_z}{\partial z} = 0$$

$$\frac{\partial u_r}{\partial t} + \frac{U_\phi}{r}\frac{\partial u_r}{\partial \phi} + U_z\frac{\partial u_r}{\partial z} - 2\frac{U_\phi u_\phi}{r} = -\frac{1}{\rho}\frac{\partial p}{\partial r}$$

$$\frac{\partial u_\phi}{\partial t} + u_r\frac{\partial U_\phi}{\partial r} + \frac{U_\phi}{r}\frac{\partial u_\phi}{\partial \phi} + \frac{u_r U_\phi}{r} + U_z\frac{\partial u_\phi}{\partial z} = -\frac{1}{\rho r}\frac{\partial p}{\partial \phi}$$

$$\frac{\partial u_z}{\partial t} + u_r\frac{\partial U_z}{\partial r} + \frac{U_\phi}{r}\frac{\partial u_z}{\partial \phi} + U_z\frac{\partial u_z}{\partial z} = -\frac{1}{\rho}\frac{\partial p}{\partial z} \qquad (4)$$

Without restricting the form of the disturbance the perturbation velocity components can be resolved into Fourier components with respect to the azimuth angle ϕ, the axial coordinate z, and time t. The perturbation velocity and p/ρ terms can be written as

$$\begin{aligned} u_r &= F(r)\exp[in\phi + i\alpha(z-ct)] \\ u_\phi &= G(r)\exp[in\phi + i\alpha(z-ct)] \\ u_z &= H(r)\exp[in\phi + i\alpha(z-ct)] \\ p/\rho &= Q(r)\exp[in\phi + i\alpha(z-ct)] \end{aligned} \qquad (5)$$

where α is real and c is complex.

Substitution in Eqs. (4) and solving gives one equivalent single equation for H

$$r^2H'' + rH' - (n^2 + \alpha^2 r^2)H = 0 \qquad (6)$$

which is the modified Bessel's function of order n having solutions $I_n(\alpha r)$ and $K_n(\alpha r)$. Exterior to the vortex sheet, the bounded solution at infinity is $K_n(\alpha r)$ while interior to the vortex sheet, the only bounded solution is $I_n(\alpha r)$. Exterior to the vortex sheet $W = -W_o$, $U_\phi = k_{1/r}$ and the solution to Eq. (6) is $H(r) = AK_n(\alpha r)$ where A is an arbitrary constant so that $P(r) = -[(W_o - c) + nk_1/\alpha r^2]\cdot AK_n(\alpha r)$ and $F(r) = -iAK_n'(\alpha r)$. Interior to the vortex sheet $W = W$, $U_\phi = -k_2/r$ and the solution to Eq. (6) is $H(r) = BI_n(r)$, where B is an arbitrary constant so that $P(r) = -[(W-c) + nk_2/\alpha r^2]BI_n(\alpha r)$ and $F(r) = -iBI_n'(\alpha r)$.

Boundary Conditions

Let the displacement at the surface of discontinuity be represented by

$$\delta = C_1 \exp[in\phi + i\alpha(z-ct)] \qquad (7)$$

The kinematic boundary condition at $r+\delta$ is given by $D\delta/Dt = u$(normal) at $r+\delta$ for the inside and the outside flows. For exterior flows, this gives

$$C\left[\alpha(W_o - c) + \frac{nk_1}{r^2}\right] = -AK_n'(\alpha r) \qquad (8)$$

and for interior flows,

$$C\left[\alpha(W-c) + \frac{nk_2}{r^2}\right] = -BI_n'(\alpha r) \qquad (9)$$

The normal stress boundary matching condition is given by

$$[P(r+\delta) + p]_{\text{outside}} = [P(r+\delta) + p]_{\text{inside}} \qquad (10)$$

where $P(r)$ is the steady pressure at r or

$$\left[P(r) + \frac{dP(r)}{dr}\delta + p\right]_{\text{outside}} = \left[P(r) + \frac{dP(r)}{dr}\delta + p\right]_{\text{inside}}$$

since the steady pressures are proportional to $1/r^3$ and should be equal across the interface, the above condition, Eq. (10), becomes

$$C\rho\frac{k_1^2}{r^3} - \rho\left[W_o - c + \frac{nk_1}{\alpha r^2}\right]Ak_n(\alpha r) = C\rho\frac{k_2^2}{r^3} - \rho\left[W - c + \frac{nk_2}{\alpha r^2}\right]BI_n(\alpha r) \qquad (11)$$

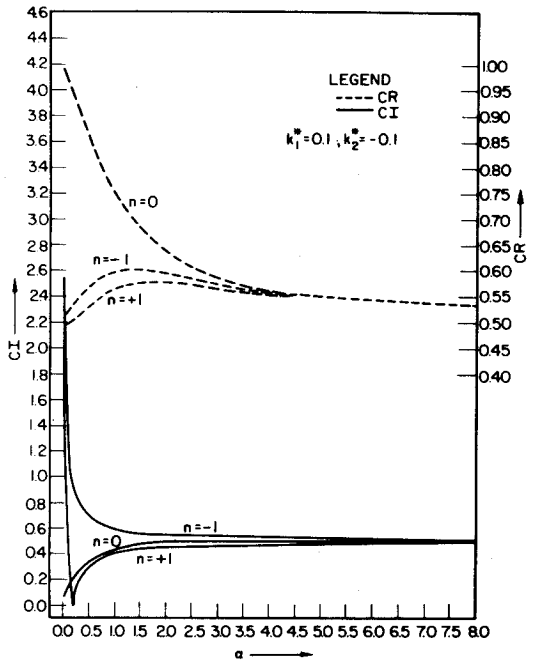

Fig. 2 Growth rates and phase velocities vs wave number for modes $n = 0, n = +1, n = -1$.

Equations (8, 9, and 11) can be solved for A, B, and C only if the following determinant equation is satisfied.

$$\alpha\left\{(W-c)+\frac{nk_2}{\alpha r^2}\right\}^2\frac{I_n(\alpha r)}{I'_n(\alpha r)}-\left(\frac{{k_1}^2-{k_2}^2}{r^3}\right)-\alpha\left\{(W_o-c)+\frac{nk_1}{\alpha r^2}\right\}^2\frac{K_n(\alpha r)}{K'_n(\alpha r)}=0$$

Solution for Growth Rates

Nondimensionalizing the stability equation, using jet velocity W and vortex sheet radius r as scaling parameters, and writing

$$k_1^* = k_1/Wr,\quad k_2^* = k_2/Wr,\quad \alpha^* = \alpha r,\quad c^* = c/W,$$
$$W_o^* = W_o/W,\quad J = I_n(\alpha^*)/I'_n(\alpha^*),\quad K = k_n(\alpha^*)/k'_n(\alpha^*)$$

the determinant equation becomes

$$a_2c^{*2}+a_1c^*+a_o=0 \tag{12}$$

where

$$a_2 = (J-K)$$
$$a_1 = 2\left\{-\left(1+\frac{nk_2^*}{\alpha^*}\right)J+\left(W_o^*+\frac{nk_1^*}{\alpha^*}\right)K\right\}$$
$$a_o = \left[\left(1+\frac{nk_2^*}{\alpha^*}\right)^2J-\left(W_o^*+\frac{nk_1^*}{\alpha^*}\right)^2K-\frac{(k_1^{*2}-k_2^{*2})}{\alpha^*}\right]$$

solving Eq. (12) for c^*

$$c^* = -a_1\pm(a_1^2-4a_2a_o)^{1/2}/2a_2 \tag{13}$$

The flow is unstable; if c^* has a positive imaginary part, i.e., $a_1^2-4a_2a_o<0$, the timewise growth rate is proportional to

$$I_m(c^*) = (4a_2a_o-a_1^2)^{1/2}/2a_2 \tag{14}$$

However, if $a_1^2-4a_2a_o>0$, $I_m(c^*)=0$, the flow is neutrally stable.

Asymptotic instability can be demonstrated by taking the limit for $\alpha^*\to\infty$. In this limit for all values of n, k_1^*, k_2^*, and W_o^*

$$c^*\to 2(1+W_o^*)\pm 2i(1-W_o^*)/4 \tag{15}$$

and since $W_o^*\ll 1$

$$\lim_{\alpha^*\to\infty} I_m(c^*) = \frac{1-W_o^*}{2}\cong 0.5$$
$$\lim_{\alpha^*\to\infty} Re(c^*) = \frac{1+W_o^*}{2}\cong 0.5$$

Physical Parameters and Computations

In most hovering cases, the helix pitch lies in the range 0.05–0.20. The helix pitch for steady velocity calculations, therefore, was chosen to be 0.1. The circumferential and axial induced velocities were computed for systems of 1–6 interdigitated vortex helices and in each case the computed velocity profiles corresponded very closely to the assumed potential flows exterior and interior to the vortex sheet. For a helix pitch of 0.1, the

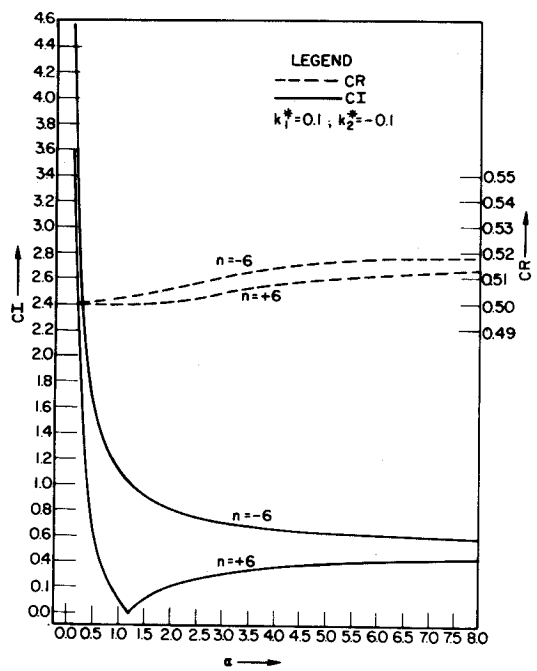

Fig. 3 Growth rates and phase velocities vs wave number for modes $n = +3, n = -3$.

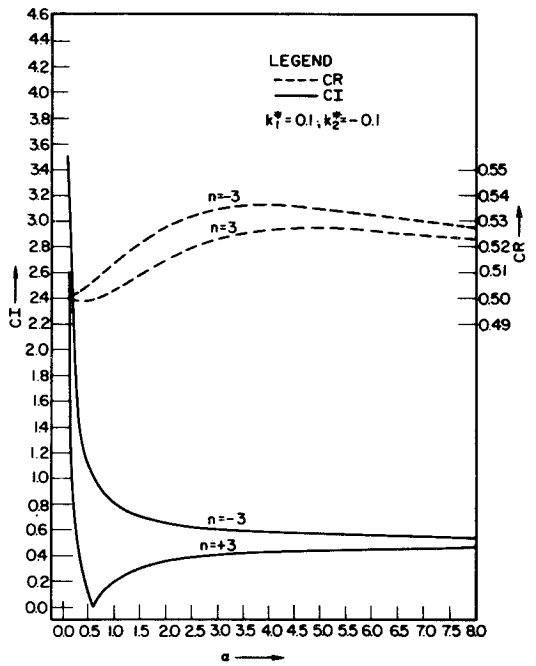

Fig. 4 Growth rates and phase velocities vs wave number for modes $n = +6, n = -6$.

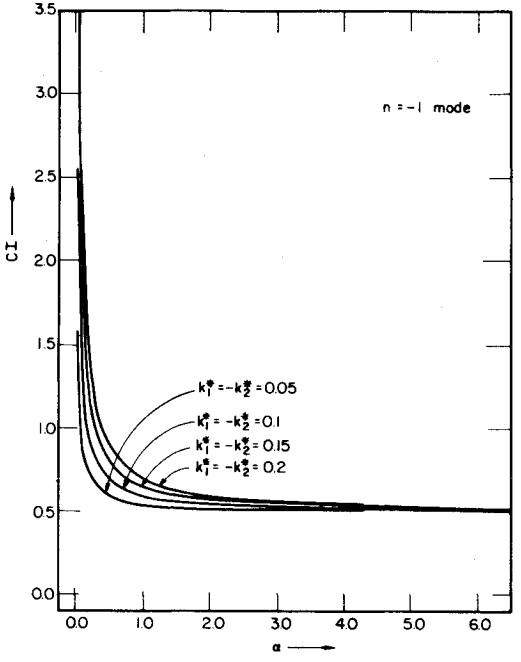

Fig. 5 Growth rates vs wave number for $n = -1$ mode for variations in the parameters k_1^* and k_2^*.

constants of the potential flow were determined to be $k_1^* = 0.1$, $k_2^* = -0.1$, and $W_o^* = -0.00043$.

Conclusions

Ponstein[5] has investigated theoretically the stability of rotating cylindrical jets, an area of considerable importance to the study of atomization phenomena in liquid jets. The present study is quite similar except that the important parameters are not the densities of the two fluids or the surface tension, but the circulation at the jet itself. For parameter values of $k_1^* = 0.1$, $k_2^* = -0.1$, and $W_o^* = 0.00043$, the following modes were analyzed for stability: $n = 0$, $n = \pm 1$, $n = \pm 2$, $n = \pm 3$, $n = \pm 4$, $n = \pm 5$, $n = \pm 6$. The growth rates $c_I = I_m(c^*)$ as a function of α^* (wave number) for some of the modes have been plotted in Figs. 2–4. c_R, which is the real part of c^* and is proportional to the wave velocities, has also been plotted.

A continuum of instabilities is found to exist. The flow is unstable for all modes and for all wavelengths except in a few cases where it is neutrally stable. The following specific conclusions can be drawn from the stability analysis. The flow is highly unstable for small α^*; i.e., large wavelength perturbations, for all the modes except for the axisymmetric mode ($n = 0$). For the $n = 0$ mode, the flow tends to be neutrally stable for very large wavelength perturbations. For large α^*, i.e., very short wavelength perturbations, the growth rate approaches 0.5 asymptotically. The n positive integer mode is relatively less unstable than the n negative integer mode. For all the positive integer modes, however, there is a point where the flow becomes neutrally stable. For the $n = 1$ mode this happens at $\alpha^* = 0.2$. For the $n = 2$ mode this point is displaced to the right; i.e., the neutral stability point occurs at higher α^* at $\alpha^* = 0.4$.

The variations of the stability characteristics with the pitch of the helix are demonstrated in Fig. 5. Higher pitch corresponds to higher rotational velocity, which means larger k_1^* and k_2^*. In this figure the $n = -1$ mode is plotted for four different values of k_1^*. The flow is more unstable for $k_1^* = 0.20$ than for $k_1^* = 0.05$ in the $n = -1$ mode. As can be seen at small and large α^* the growth rates are relatively insensitive to changes in k_1^*. For the $n = 0$ mode the growth rates are not found to vary with changes in k_1^*.

References

[1] Gupta, B. P. and Loewy, R. G., "Theoretical Analysis of the Aerodynamic Stability of Multiple, Interdigitated Helical Vortices," *AIAA Journal*, Vol. 12, Oct. 1974, pp. 1381–1387.

[2] Lessen, M., Deshpand, N. V., and Ohanes, B. H., "Stability of a Potential Vortex with a Nonrotating and Rigid-Body Rotating Top-Hat Jet Core," *Journal of Fluid Mechanics*, Vol. 60, Sept. 1973, pp. 459–466.

[3] Oberoi, M. S., Chow, C. Y., and Nanan, J., "Stability of Jets," *Physics of Fluids*, Vol. 15, 1972, pp. 1718–1727.

[4] Batchelor, G. K. and Gill, A. E., "Analysis of the Stability of the Axisymmetric Jets," *Journal of Fluid Mechanics*, Vol. 14, Dec. 1962, pp. 529–557.

[5] Ponstein, J., "Instability of Rotating Cylindrical Jets," *Applied Science Research*, Sec. A, Vol. 8, 1959, pp. 425–456.